Malaysian Journal of Microbiology, Vol 18(4) 2022, pp. 354-369
DOI: http://dx.doi.org/10.21161/mjm.221396

Malaysian Journal of Microbiology
Published by Malaysian Society for Microbiology
(In SCOPUS since 2011)

Mycosynthesis of thermostable silver nanoparticles by the endophytic *Albifimbria verrucaria* with antimicrobial and antiproliferative activities

Mina Nasry Zaky*, Noha Mohamed Abd Elhameed, Adel A. El Mehalawy and Samar Samir Mohamed

Microbiology Department, Faculty of Science, Ain Shams University, 11566, Abbassia, Cairo, Egypt.
Email: mina-nasry@hotmail.com

Received 5 January 2022; Received in revised form 22 April 2022; Accepted 9 May 2022

ABSTRACT

Aims: This study was aimed to screen and isolate soil and endophytic fungi with the ability to biosynthesize stable silver nanoparticles (SNPs) with antimicrobial and antiproliferative activities.
Methodology and results: A total of 60 fungal isolates isolated from soil and plant samples were screened for their ability to biosynthesize SNPs. Among which, 21 isolates have supported the biosynthesis of SNPs. Furthermore, the endophytic isolate PRR_2.1 synthesized highly thermostable SNPs with long shelf life. The PRR_2.1 isolate was identified as *Albifimbria verrucaria* by morphological and molecular means. The synthesis of SNPs was initially monitored by UV-Vis spectroscopy. Further characterization by transmission electron microscopy, X-ray diffraction and dynamic light scattering revealed well-dispersed spherical crystalline in nature SNPs with a mean size of 14 nm and zeta potential of –24.47 mV. Fourier transform infrared spectroscopy showed the presence of biomolecules adsorbed on the surface of biosynthesized SNPs responsible for their synthesis and stability. The mycosynthesized SNPs exhibited stronger antifungal activity against pathogenic strains of *Aspergillus niger*, *A. flavus*, *A. fumigatus* and *Candida albicans* with respect to its antibacterial activity against *Escherichia coli*, *Staphylococcus aureus*, *Bacillus cereus* and *Klebsiella pneumoniae* compared to standard antifungal itraconazole and antibiotic cefadroxil with mostly consistent minimum inhibitory concentration of 5.31 µg/mL. The biosynthesized SNPs demonstrated dose-dependent *in vitro* antiproliferative activity against cancerous HeLa cell line with IC_{50} value of 2.52 µg/mL and less cytotoxic activity against WI-38 (normal human lung fibroblasts) cell line with CC_{50} value of 10.2 µg/mL.
Conclusion, significance and impact of study: These results show the potential of endophytic fungi biosynthesized SNPs as possible biofriendly, safe and efficient antimicrobial agents with promising antiproliferative activity and low cytotoxicity, which can be furtherly implemented in various biomedical and biotechnological applications.

Keywords: Albifimbria verrucaria, antiproliferative, antimicrobial, endophytic mycosynthesis, silver nanoparticles

INTRODUCTION

In the last few years, there has been a worldwide trend for green synthesis of nanoparticles which has proven to be safer, simpler, more cost-effective and more eco-friendly than otherwise physical or chemical approaches (Rauwel *et al*., 2015). The use of nanoparticles has become widespread because of their evident roles in many applications, whether medical, biotechnological, or industrial. This includes their role as antimicrobial agents; their applications in medical devices such as in catheters, wound dressing and bone cement; as well as their wide range of biotechnological and industrial applications involving water purification, biosensors, bioimaging, antimicrobial paint, catalytic activity, etc. (Khatoon *et al.*, 2017). The size of nanoparticles has gained them all sorts of physical properties differing from those of their original parent materials, which pronounced their potent properties especially in human health care (Burşuel *et al*., 2018; Lee and Jun, 2019).

The recruitment of microorganisms as cell-factories for the synthesis of nanoparticles has been scientifically favored over the past decade. A wide array of microorganisms, including algae, actinomycetes, bacteria, filamentous fungi and yeasts have been the subject of study for the synthesis of nanoparticles (Adeeyo and Odiyo, 2018; Dhabalia *et al*., 2020). Out of which, fungi have become the center of attention for the biosynthesis of nanoparticles due to their bio-advantages, such as they are fastidious to grow producing a large amount of biomass in a short period of time, easy to handle, their ability to withstand agitation and flow pressure in bioreactors and their ability to produce a battery of extracellular secondary metabolites of enzymes and proteins which enable them of rapid reduction of metal ions to nanoparticles (Abdel-Rahim *et al*., 2017). The

*Corresponding author

ISSN (print): 1823-8262, ISSN (online): 2231-7538

Malays. J. Microbiol. Vol 18(4) 2022, pp. 354-369
DOI: http://dx.doi.org/10.21161/mjm.221396

fungal extracellular synthesis of silver nanoparticles is more time-efficient and does not require further processing steps compared to intracellular synthesis (Ghareib *et al*., 2016), which is the reason why the fungal mediated extracellular synthesis of nanoparticles is considered to be the ideal choice for high productivity and yield of nanoparticles (Saxena *et al*., 2016; El-Eraky *et al*., 2017).

Although there are many published studies involving the biogenic synthesis of silver nanoparticles (SNPs), the exact mechanism of synthesis isn't fully understood yet. It is well established that mycosynthesis of silver nanoparticles occurs as a result of the reaction between enzyme(s) present in fungal filtrate acting as a reductant of ionic silver to produce elemental silver at nanometric size (Guilger-Casagrande and de Lima, 2019). The size of biosynthesized SNPs depends on various conditions such as fungal species, temperature, pH, dispersion media and the presence of a capping agent (Khandel and Shahi, 2018). Several biomolecules can react with silver ions during the synthesis process, such as those involved in complex pathways associated with the conversion of NADPH/NADH to $NADP^+$/NAD^+ (Gudikandula *et al*., 2017). NADH and NADH-dependent nitrate reductase enzymes are of the most importance in the biosynthesis of SNPs (Baymiller *et al*., 2017). Hietzschold *et al*. (2019) showed that the biosynthesis of SNPs was carried out solely by NADPH without the need for a nitrate-reductase enzyme. Other studies have reported the successful synthesis of silver nanoparticles via various soil as well as endophytic fungal species such as *Fusarium oxysporum* which has successfully synthesized silver nanoparticles through the production of NADH-dependent nitrate reductase enzyme (Rai *et al*., 2021). The endophytic *fungus Phomopsis liquidambaris* isolated from leaves of *Salacia chinensis* plant synthesized stable silver nanoparticles (Seetharaman *et al*., 2018), the marine fungus *Penicillium fellutanum* isolated from coastal mangrove sediment in south India enabled the rapid synthesis of silver nanoparticles (Kathiresan *et al*., 2009) and the non-pathogenic soil fungus *Trichoderma viride* was used for the production of silver nanoparticles (Manikandaselvi *et al*., 2020).

Many factors such as over-prescription of antibiotics, patients not finishing the entire antibiotic course, the overuse of antibiotics in livestock and fish farming, poor infection control in health care settings and the absence of new antibiotics being discovered have given rise to increased incidence of microbial resistance to antibiotics which urges the seek after and development of new effective antimicrobial agents (Su *et al*., 2018; Duval *et al*., 2019). Silver nanoparticles have shown promising antimicrobial activity against a broad spectrum of microorganisms such as Gram-positive and Gram-negative bacteria, including multidrug-resistant human pathogens as well as pathogenic fungi without the ability of the microorganism to develop resistance against them. Silver nanoparticles biosynthesized from endophytic *Fusarium* sp. isolated from medicinal plant *Withania somnifera* demonstrated potent antibacterial activity against *Escherichia coli*, *Staphylococcus aureus* and *Salmonella typhi* (Singh *et al*., 2015). Biosynthesized silver nanoparticles using *Aspergillus sydowii* showed effective antifungal activity against several *Candidas* and pathogenic *Aspergilli* species (Wang *et al*., 2021); green synthesized silver nanoparticles using *Melia azedarach* leaf extract exhibited *in vitro* and *in vivo* antifungal activity against *Verticillium dahliae* wilt of eggplant (Jebril *et al*., 2020). Silver nanoparticles have also been used in combination with different antibiotics in a synergistic manner to enhance their antimicrobial activity (Abushiba *et al*., 2019).

Many studies have reported potent antiproliferative activity of biosynthesized silver nanoparticles against different cancerous cell lines such as HCT116 (human colorectal carcinoma), A549 (human lung carcinoma), MCF7 (human Caucasian breast adenocarcinoma) and PC3 (prostate cancer) cell lines (Othman *et al*., 2019).

As part of our effort in this study, we aim to screen for fungi of different sources, including endophytic and soil with the ability of biosynthesis of stable silver nanoparticles with antimicrobial activity and antiproliferative potential.

MATERIALS AND METHODS

Chemicals

High-quality analytical grade silver nitrate ($AgNO_3$) was purchased from Sigma-Aldrich Co., St Louis, MO, USA. Microbiological grade agar was purchased from B&V srl, Italy. Malt extract, yeast extract, glucose and peptone were purchased from Alpha Chemicals Pvt. Ltd, India. Potato infusion prepared from 200 gm grated potatoes boiled in 1 liter of water.

Sample collection

Ten samples were collected. Three soil samples were collected from different saline arid regions near Lake Moeris (Qarun Lake) in the northwest area of Faiyum Oasis located southwest of Cairo Governorate, Egypt. Seven plants, three of which are fennel (*Foeniculum vulgare)*, mint (*Mentha longifolia)* and basil *(Ocimum basilicum)* were isolated from cultivated high salinity lands alongside Lake Moeris. The other four plants are camelthorn bush (*Alhagi graecorum)*, Phog (*Calligomum polygonoids*), nitric bush (*Nitraria retusa*) and *Tetraena alba* (*Zygophyllum album*) were isolated from the arid highly saline subtropical region of Wadi El-Rayan Protectorate, Faiyum Governorate, Egypt.

Isolation of fungi

Isolation of soil fungi

Ten grams of each soil sample were suspended in 500 mL sterile distilled water, then shaken thoroughly for 30 min and left to settle for another 30 min. After which, 1 mL of supernatant water was spread with a sterile glass

 ISSN (print): 1823-8262, ISSN (online): 2231-7538

Malays. J. Microbiol. Vol 18(4) 2022, pp. 354-369
DOI: http://dx.doi.org/10.21161/mjm.221396

spreader on the surface of three isolation media: potato dextrose agar, malt extract agar and hyper-osmotic medium amended with chloramphenicol to inhibit bacterial growth (Pelhate, 1968). Three Petri-dishes of each isolation medium were inoculated with each soil sample, two sets of petri-dishes were inoculated for incubation at 28 °C and 37 °C for seven days, and grown colonies were purified and maintained on PDA slants.

Isolation of endophytic fungi

The collected plants were extensively washed to remove any residual dirt, then left in the air to dry, after which, each plant tissue (roots, stems and leaves) was cut with a sterile scalpel into small segments about 1 cm each to undergo surface sterilization through sequential immersion in 96% ethanol (C_2H_5OH) for 1 min, 2% sodium hypochlorite (NaClO) for 3 min, 96% ethanol for 30 sec, followed by repeated rinsing in sterile distilled water to remove any leftover sterilizing agent (Sieber *et al*., 1988; Crous *et al*., 1995). Three segments of each plant tissue were placed on the surface of these isolation media; potato dextrose agar (PDA) and malt yeast extract agar (MYEA) amended with chloramphenicol to inhibit bacterial growth. Three isolation Petri-dishes were made for each plant tissue. 1 mL of the sterile distilled water used in the final rinsing step of the surface sterilization method was also spread on the surface of the same media mentioned above to ensure that the grown isolates are indeed endophytes and not contamination. The cultured plates were incubated at 28 °C for 7 to 14 days and monitored at equal time intervals. The tissue-emerged individual fungal colonies were purified and maintained on PDA slants for further use.

Screening for fungal isolates with the ability of silver nanoparticles biosynthesis

A total of 60 fungal isolates were screened for their biogenic ability of silver nanoparticles. Each of 60 fungal isolates was grown on potato dextrose broth (PDB) in Erlenmeyer flask and incubated at 28 °C for 7 days in a shaking incubator (120 rpm), after which the grown fungal biomass was removed from the broth medium by means of gravity filtration through Whatman filter paper No.1 and extensively washed with sterile distilled water to remove any residual components of broth medium. Ten grams (wet weight) of fungal biomass was brought in contact with 100 mL sterile deionized water in an Erlenmeyer flask and incubated for 48 h under the same conditions, the fungal biomass free filtrate was obtained through gravity filtration with Whatman filter paper No.1, 100 mL of fungal-free filtrate was reacted with a known amount of silver nitrate (17 mg) to yield an overall concentration of 10^{-3} M Ag^+ ions while the biomass free filtrate and silver nitrate solution were kept as controls. The reaction mixture was maintained in the dark at room temperature and the change in color of the reaction mixture was monitored over 48 h period (Balakumaran *et al*., 2016).

Identification of fungal isolates

Out of the 60 fungal isolates screened, those which have successfully supported the extracellular synthesis of silver nanoparticles were identified. The identification of fungal isolates was done at the species level based on the morphology of fungal culture and microscopic characteristics (slide culture technique) according to Moubasher (1993).

Molecular identification of the most significant fungal isolate

Among the fungal isolates that were able to synthesize silver nanoparticles, isolate $PRR_2.1$ fabricated highly stable silver nanoparticles was selected for further molecular identification. The fungal genetic material was extracted using Zymo-Spin™ Technology, followed by PCR amplification using ITS1 (forward 5' TCCGTAGGTGAACCTGCGG 3') and ITS4 (reverse 5' TCCTCCGCTTATTGATATGC 3') primers (White *et al*., 1990). ITS1-5.8S-ITS2 ribosomal DNA region sequence was amplified. The purification of the PCR product was performed using ZYMO RESEARCH DNA clean-up and concentrator kits. The extraction of fungal genetic material and the purification of PCR products were carried out by Sigma Scientific Services Co., Egypt. The pure amplified PCR product was sequenced by ABI 3730xl DNA sequencer using Sanger technology at GATC Biotech AG., Konstanz, Germany. The amplified fungal DNA sequence was aligned with reference sequences from the NCBI database using MEGA-X software to construct a maximum likelihood phylogenetic tree (Mousa *et al*., 2021). The fungal isolate $PRR_2.1$ was submitted at GenBank and was also deposited at Culture Collection Ain Shams University (CCASU) located at the Faculty of Pharmacy, Ain Shams University.

Effect of different parameters on silver nanoparticles biosynthesis

One factor at a time method was employed to investigate several reaction parameters for optimal biosynthesis of silver nanoparticles such as different growth media, including potato dextrose broth (PDB), Czapek Dox broth (CDB), Sabouraud dextrose broth (SDB) and Malt Glucose Yeast Peptone broth (MGYPB) were examined for their potential to support the best production of fungal biomass and silver-reducing biomolecules. Different concentrations of fungal biomass 10, 15, 20, 25 and 30 grams/100 mL deionized water were tested for optimal synthesis of silver nanoparticles; different concentrations of silver nitrate 0.5, 1, 1.5, 2, 2.5 and 3 mM were added to fungal-free filtrate which was incubated at different pH values ranging from 3 to 10 and different temperatures ranging from 30 °C to 110 °C up to 48 h incubation period (Mishra *et al*., 2014).

 ISSN (print): 1823-8262, ISSN (online): 2231-7538

Malays. J. Microbiol. Vol 18(4) 2022, pp. 354-369
DOI: http://dx.doi.org/10.21161/mjm.221396

Characterization of biosynthesized silver nanoparticles

UV-Visible spectroscopy

Successful synthesis of silver nanoparticles was initially observed visually as a color change of the reaction mixture to reddish-brown due to reduction of silver ions to atomic silver (Basavaraja *et al*., 2008), followed by subsequent confirmation using Thermo Scientific Evolution 201 UV-Vis spectrophotometer to scan the absorbance spectra wavelength of silver nanoparticles ranging from 300 to 700 nm with a resolution of 1 nm.

High-resolution transmission electron microscopy

The size and morphology of silver nanoparticles were detected using (JEOL JEM-2100) HR-TEM at National Research center (NRC), Egypt. The sample was prepared by placing a 10 µL droplet of silver nanoparticles solution on a carbon-coated copper grid, left to be air-dried at room temperature (Tyagi *et al*., 2019). The micrographs were generated at 120 kV and the analysis of selected area electron diffraction (SAED) was performed.

Dynamic light scattering

The average hydrodynamic particle size distribution and zeta potential were measured by DLS (Ahmad *et al*., 2015) using Nicomp ZLS380 (USA) zeta-sizer at NRC, Egypt; size measurements were carried out at 30 °C and a wavelength of 632 nm.

Fourier transform infrared spectroscopy

The biosynthesized silver nanoparticles dispersion was centrifuged at 13,000 rpm/20,000 g for 30 min; the resultant pellet was resuspended in 1 mL ethyl alcohol and centrifuged again for 30 min; ethyl alcohol was left to evaporate and the air-dried silver nanoparticle pellet was used to perform FTIR spectroscopy by Bruker Alpha II FTIR spectrophotometer (Opus 7.8 software) to figure out the functional groups present in potential biomolecules responsible for synthesis and stabilization of silver nanoparticles (Farsi and Farokhi, 2018). The FTIR spectroscopy was carried out in the range of 400-4000 cm^{-1} with a resolution of 4 cm^{-1} at Central Laboratory, Ain Shams University, Egypt.

X-ray diffraction analysis

The crystalline nature of biosynthesized silver nanoparticles was examined using Empyrean X-ray diffractometer, Malvern PANalytical at NRC, Egypt to scan X-ray diffraction pattern using Cu Kα radiation, λ=1.5405 Å, over a range of Bragg angles 2θ between 20° and 80° at 60 kV, 50 mA (Jyoti *et al*., 2016).

***In vitro* antimicrobial activity of silver nanoparticles**

Agar well diffusion method

The antimicrobial activity of mycosynthesized silver nanoparticles was evaluated using agar well diffusion assay (Pongtharangkul and Demirci, 2004; El-Sayed *et al*., 2020) against eight human pathogens: *Escherichia coli* ATCC 35218, *Staphylococcus aureus* ATCC 29213, *Klebsiella pneumoniae* ATCC 70060, *Bacillus cereus* ATCC 14579, *Candida albicans*, *Aspergillus flavus*, *Aspergillus fumigatus* and *Aspergillus niger*. The tested pathogens' inoculums were prepared in 0.85% saline (Petrikkou *et al*., 2001; Balouiri *et al*., 2016); the bacterial and yeast inoculums were adjusted spectrophotometrically according to the Clinical and Laboratories Standards Institute (CLSI) to equate the optical density of 0.5 McFarland standard of 0.08-0.12 at wavelength 625 nm (OD625) which is equivalent to 1-2 × 10^8 CFU/mL for bacteria and 1-5 × 10^6 CFU/mL for *Candida albicans*, while for *Aspergillus* spp., the optical density at 530 nm (OD530) was adjusted between 0.03 and 0.5 equivalent to 1-5 × 10^6 CFU/mL (Petrikkou *et al*., 2001). The prepared inoculums of test pathogens were surface inoculated on Muller-Hinton agar (MHA), four wells (6 mm in diameter) were made per Petri-dish loaded with: (i) 100 µL of silver nanoparticles (170 µg/mL), (ii) 100 µL of cefadroxil antibiotic (100 µg/mL) for bacterial pathogens while 100 µL of itraconazole (100 µg/mL) solubilized in dimethyl sulfoxide (DMSO) for fungal pathogens as positive control, (iii) Mycelial-free filtrate to rule out any potential antimicrobial activity that it may possess and (iv) $AgNO_3$ solution (100 µg/mL), the inoculated plates were incubated at 37 °C for 24 h in case of bacteria and at 28 °C for 48 h in case of fungi, after which, zones of inhibition (ZOI) were precisely measured and the results were recorded in millimeters, the experiment was carried out in triplicate and the mean results were taken.

The minimum inhibitory concentration of biosynthesized silver nanoparticles

The determination of minimum inhibitory concentration (MIC) of silver nanoparticles was carried out using broth micro-dilution method according to CLSI using 96 well microplates (Singh *et al*., 2013; Balouiri *et al*., 2016), in which two-fold serial dilutions of noted concentrations of silver nanoparticles (85, 42.5, 21.25, 10.62, 5.31, 2.66, 1.32, 0.66, 0.33 and 0.16 µg/mL), antibiotic/antifungal and silver nitrate (50, 25, 12.5, 6.25, 3.12, 1.56, 0.78, 0.39, 0.19 and 0.09 µg/mL) were made each in 100 µL of either; nutrient broth (in case of bacteria) and PDB (in case of fungi) in wells 1 to 10, with well No.11 (broth media only) and well No.12 (inoculated broth media without antimicrobial agent) kept as controls. 50 µL microbial inoculum equivalent to 0.5 McFarland standard was added to wells 1-10 and 12, the microplates were incubated at an appropriate temperature (37 °C/24 h for bacteria and 28 °C/48 h for fungi), after which the MIC

 ISSN (print): 1823-8262, ISSN (online): 2231-7538

Malays. J. Microbiol. Vol 18(4) 2022, pp. 354-369
DOI: http://dx.doi.org/10.21161/mjm.221396

Table 1: Fungal isolates supporting biosynthesis of silver nanoparticles.

Isolate no.	Isolate name	Identification	Source
1	PRR_2.1	*Albifimbria verrucaria*	*Ocimum basilicum* roots
2	MRR_2	*Aspergillus aculeatus*	*Ocimum basilicum* roots
3	B.MEX_3	*Aspergillus aculeatus*	Soil sample (B)
4	B.HO_1 ORG.2 28 °C	*Aspergillus alutaceus*	Soil sample (B)
5	B.HO_2 ORG.2 28 °C	*Aspergillus alutaceus*	Soil sample (B)
6	A.MEX_1 ORG.1 28 °C	*Aspergillus clavatus*	Soil sample (A)
7	A.H_3 ORG.2 37 °C	*Aspergillus nidulans*	Soil sample (A)
8	A.PDA ORG.1 28 °C	*Aspergillus nidulans*	Soil sample (A)
9	A.PDA_3 ORG.1 28 °C	*Aspergillus niger*	Soil sample (A)
10	Plant (B) MYE Stems 2	*Aspergillus niger*	*Zygophyllum album* stems
11	Plant (D) PDA Stems 1	*Aspergillus sydowii*	*Alhagi graecorum* stems
12	A.H_3 ORG.1 37 °C	*Aspergillus terreus* var. *terreus*	Soil sample (A)
13	A.H_3 ORG.2 28 °C	*Aspergillus terreus* var. *terreus*	Soil sample (A)
14	Plant (B) MYE Stems 3	*Aspergillus terreus* var. *terreus*	*Zygophyllum album* stems
15	Plant (C) MYE Stems 2	*Aspergillus terreus* var. *terreus*	*Calligonum polygonoids* stems
16	Plant (C) MYE Stems 1	*Candida* sp.	*Calligonum polygonoids* stems
17	PNR_1.1	*Chrysosporium tropicum*	*Mentha longifolia* roots
18	Plant (A) PDA Leaf 1	*Fennelia nivea*	*Nitraria retusa* leaves
19	Plant (C) MYE Stems 1	*Penicillium* sp.	*Calligonum polygonoids* stems
20	A.H_1 ORG.3 37 °C	*Scopulariopsis brumptii*	Soil sample (A)
21	Plant (B) MYE Stems 1	*Yellow sterile mycelium*	*Zygophyllum album* stems

was recorded visually as the lowest concentration of antimicrobial agent that completely inhibited microbial growth.

In vitro antiproliferative and cytotoxicity evaluation of biosynthesized silver nanoparticles

The cytotoxic activity of silver nanoparticles was evaluated against WI-38 cell line (normal human lung fibroblasts obtained from VACSERA Tissue Culture Unit) and its antitumor potential was assessed against HeLa cell line (human cervical cancer) obtained from American Type Culture Collection (ATCC, Rockville, MD) using MTT assay. The optical density was measured with the microplate reader (SunRise, TECAN Inc, USA) at 590 nm to determine the number of viable cells and estimate the 50% inhibitory concentration (IC_{50}, the concentration of silver nanoparticles that inhibits proliferation of HeLa cells by 50%) and the cytotoxic concentration (CC_{50}, the concentration of silver nanoparticles that causes death of 50% of the tested WI-38 cellular population) values through graphical plots of the dose-response curve for each conc. using Graphpad Prism software (San Diego, CA, USA) (Mosmann, 1983), the cytotoxicity assay was performed at the Regional Center for Mycology and Biotechnology, Al-Azhar University.

RESULTS

Isolation, screening and identification of fungal isolates with the biogenic ability of silver nanoparticles

A total of 60 fungal isolates were isolated from 3 soil samples and seven plant specimens, were screened for their ability to synthesize silver nanoparticles; among which, 21 isolates had the ability to synthesize silver nanoparticles. Positive silver nanoparticles synthesizing isolates were identified by means of morphological and microscopic characteristics (Table 1). Furthermore, the endophytic fungal isolate PRR_2.1 isolated from *O. basilicum* roots was able to synthesize very stable silver nanoparticles that have shown long-term stability for 4 months without the tendency of aggregation. Therefore, isolate PRR_2.1 was selected for further molecular identification and optimization procedures. The morphological appearance of 7 days old culture of isolate PRR_2.1 as observed on PDA, shows white mycelium with a buff reverse and spore aggregations ranging from dark olive to black color embedded in white mycelium (Figure 1a). The microscopic examination of isolate PRR_2.1 shows hyphae and elongated conidia lacking fantail appendages (Figure 1b). Both morphological characteristics and microscopic examination of PRR_2.1 isolate provided its preliminary identification as *Albifimbria* sp. (Weaver *et al*., 2021).

Molecular identification

The alignment of the PCR amplified ITS1-5.8S-ITS2 sequence of isolate PRR_2.1 with reference sequences at the NCBI database, along with its morphological and microscopic characteristics (Figure 1a and 1b) confirmed it to be *Albifimbria verrucaria*. Maximum likelihood phylogenetic tree was constructed, showing its closely related strains (Figure 1c). *A. verrucaria* isolate PRR_2.1 was submitted at the GenBank database under accession number MW890761 and was also deposited at CCASU under strain numbers CCASU-2021 F1.

 ISSN (print): 1823-8262, ISSN (online): 2231-7538

Malays. J. Microbiol. Vol 18(4) 2022, pp. 354-369
DOI: http://dx.doi.org/10.21161/mjm.221396

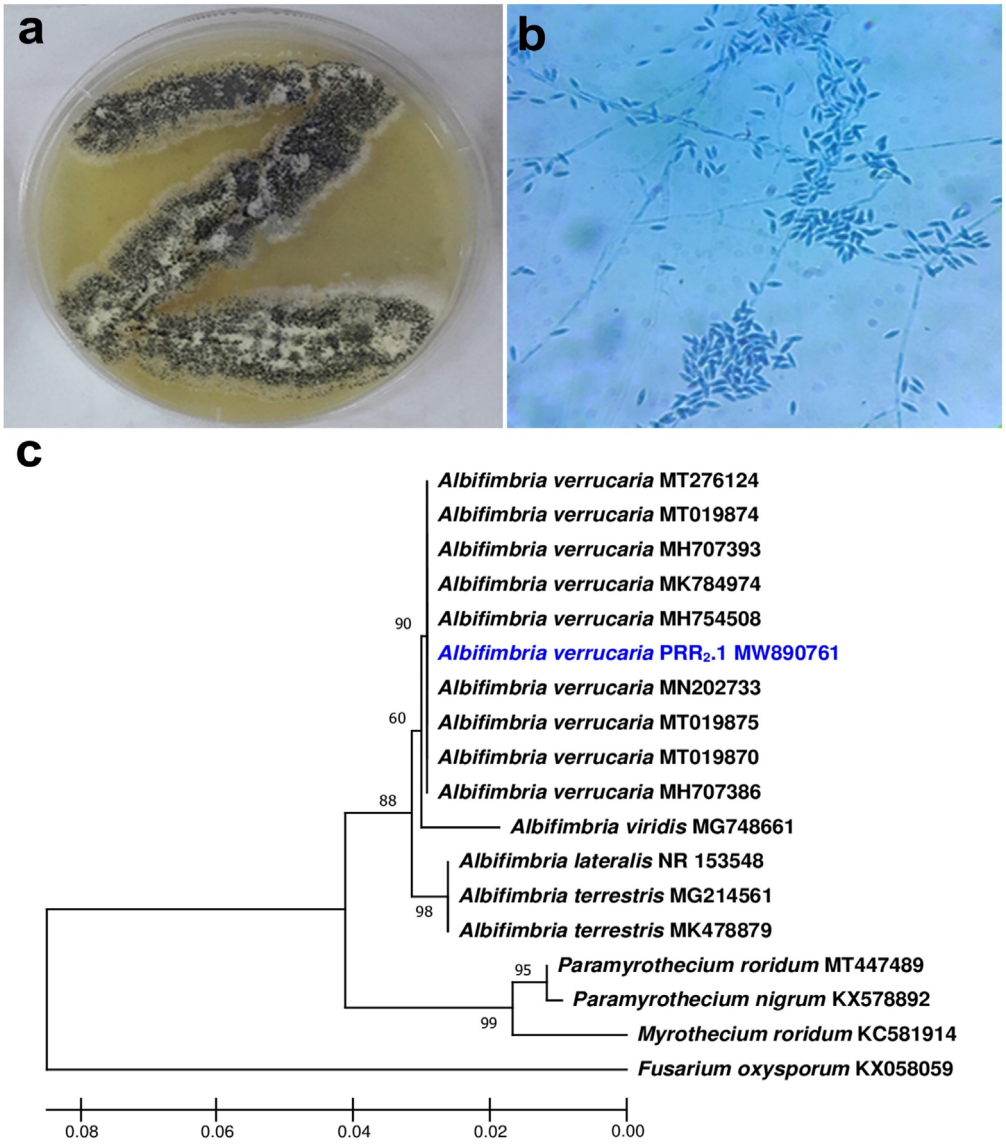

Figure 1: Morphological characteristics and molecular identification of *Albifimbria verrucaria* PRR$_2$.1. (a) Macroscopic morphology of 7 days old culture as observed on PDA. (b) Microscopic morphology (640×) showing conidia and conidiophores. (c) Phylogenetic tree of *A. verrucaria* PRR$_2$.1 (MW890761) showing closely related strains based on ITS1-5.8S-ITS2 DNA sequence.

Effect of different reaction parameters on silver nanoparticles synthesized by *Albifimbria verrucaria* PRR$_2$.1

Albifimbria verrucaria isolate PRR$_2$.1 was used for optimizing the synthesis of silver nanoparticles. Different reaction parameters such as concentrations of fungal biomass, concentrations of silver nitrate, growth media, pH and incubation temperatures were investigated. UV-Vis spectrophotometry was employed to study the effect of each of the aforementioned conditions for the optimal synthesis of silver nanoparticles. Among the different concentrations of fungal biomass tested, 15 g/100 mL supported the synthesis of the highest concentration of silver nanoparticles (the highest surface plasmon resonance intensity) whereas 20 g/100 mL supported the synthesis of nanoparticles with the smallest size as observed with absorption spectrum exhibiting blue shift compared with the spectra of other biomass concentrations (Figure 2a). Among the different molar concentrations of silver nitrate examined, 1.5 mM supported the synthesis of silver nanoparticles with the highest concentration and smallest size (Figure 2b). As for the different growth, media tested, only PDB had the ability to induce the maximum production of fungal biomass as well as silver nanoparticles, while the other

 ISSN (print): 1823-8262, ISSN (online): 2231-7538

Malays. J. Microbiol. Vol 18(4) 2022, pp. 354-369
DOI: http://dx.doi.org/10.21161/mjm.221396

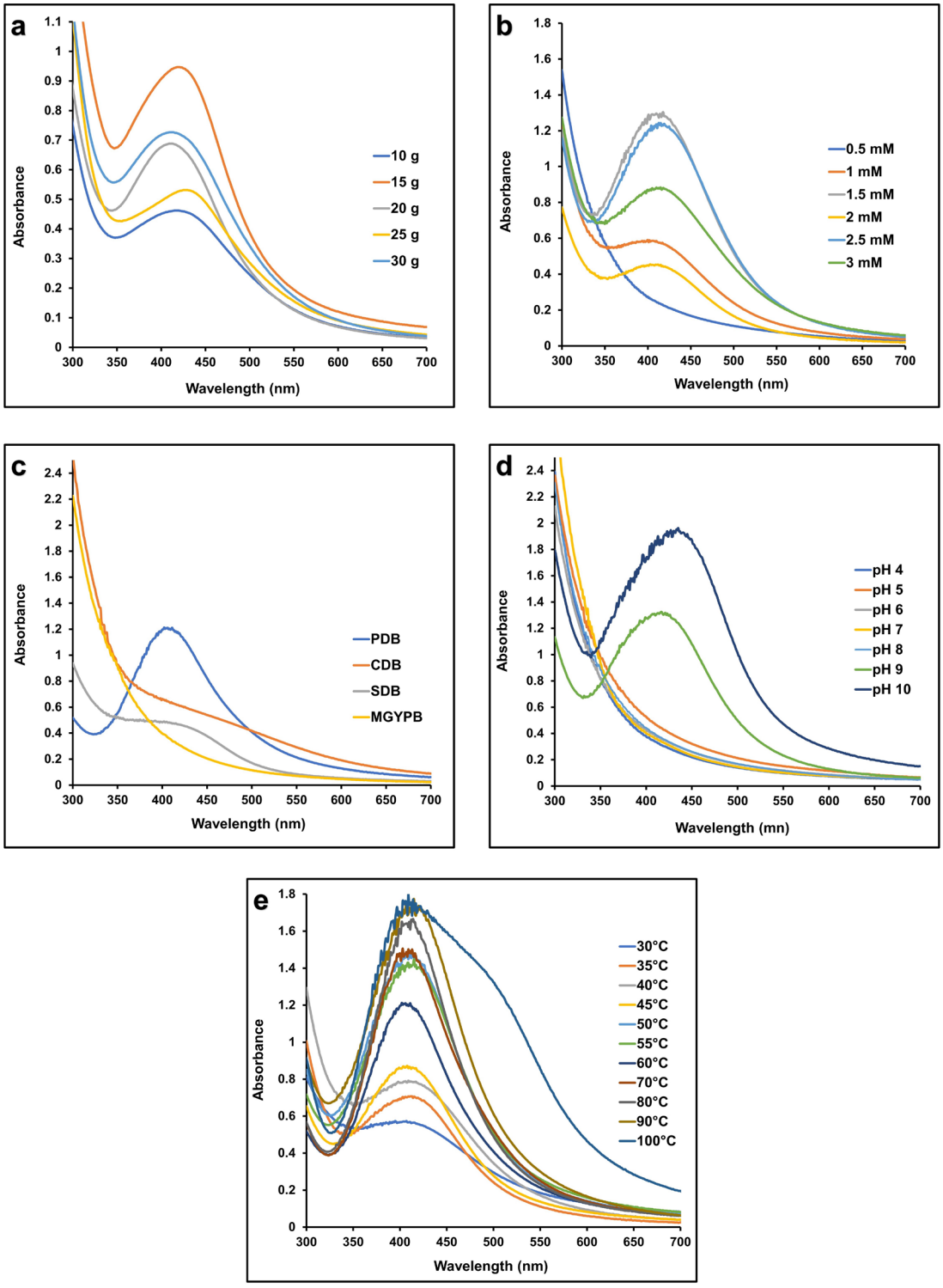

Figure 2: Optimization of silver nanoparticles synthesized by *A. verrucaria* PRR$_2$.1. (a) Effect of biomass concentration (5-30 g/100 mL) of *A. verrucaria* PRR$_2$.1 on synthesis of silver nanoparticles. (b) Effect of different molar concentrations of silver nitrate (0.5-3 mM) on synthesis of silver nanoparticles. (c) Effect of different growth media on synthesis of silver nanoparticles. (d) Effect of pH (4-10) on the synthesis of silver nanoparticles. (e) Effect of temperature (30-100 °C) on synthesis of silver nanoparticles.

 ISSN (print): 1823-8262, ISSN (online): 2231-7538

Malays. J. Microbiol. Vol 18(4) 2022, pp. 354-369
DOI: http://dx.doi.org/10.21161/mjm.221396

media tested inhibited the synthesis process (Figure 2c). It was found that only alkaline pH values (pH 9-10) were able to support the successful synthesis of silver nanoparticles with no observed color change at lower pH values (pH 3-8), indicating inhibition of synthesis (Figure 2d). As the incubation temperature of the reaction mixture increased, the rate of synthesis was found to increase in a directly proportional manner up to 100 °C, with a blue shift in absorption spectrum observed at 60 °C (Figure 2e). No synthesis of silver nanoparticles was observed at 110 °C. In the light of these results, the optimal conditions selected for the synthesis of the highest concentrations with the smallest size SNPs were PDB as growth media, 20 g/100 mL fungal biomass, 1.5 mM silver nitrate, pH ranging between 9-10 and 60 °C as the incubation temperature of the reaction mixture.

Characterization of optimized silver nanoparticles synthesized using *Albifimbria verrucaria* PRR$_2$.1

UV-Vis spectroscopy

The initial indication of synthesis of silver nanoparticles was observed as a change in color of the reaction mixture to reddish-brown, while the fungal-free filtrate and silver nitrate solution used as controls retained their initial colors. This change in color is due to the excitation of surface plasmon resonance (SPR) which is a characteristic aspect of nanoparticles (Bhangale *et al.*, 2019; Lee and Jun, 2019). The absorption spectrum peak of optimized silver nanoparticles synthesized using *A. verrucaria* PRR$_2$.1 was recorded at 410 nm (Figure 3), which had confirmed the synthesis of silver nanoparticles.

High-resolution transmission electron microscopy and dynamic light scattering

HR-TEM micrographs of silver nanoparticles synthesized via *A. verrucaria* PRR$_2$.1 (Figure 4a, 4b and 4c) confirmed synthesis of well-dispersed spherical shaped nanoparticles with diameters ranging between 1-12 nm. Insert of Figure 4b shows SAED pattern. Dynamic light scattering (DLS) revealed mean size of silver nanoparticles synthesized by *A. verrucaria* PRR$_2$.1 as 14 nm (Figure 4d) and their zeta potential as –24.47 mV (Figure 4e).

FTIR spectroscopy and XRD analysis

The FTIR spectrum of silver nanoparticles synthesized by *A. verrucaria* PRR$_2$.1 showed clear absorption peaks at 3266, 2981, 2932, 1640 and 1043 cm^{-1} (Figure 4f), indicating functional groups of possible biomolecules responsible for synthesis and capping of silver nanoparticles. The strong, broad peak at 3266 cm^{-1} corresponds to O-H (hydroxyl) stretching in alcohols, phenols and flavonoid compounds. The peaks at 2981 and 2932 cm^{-1} corresponds to C-H (sp^3 hybridization) stretching vibration. C=O (carbonyl) stretch in N-C=O amide group of peptide bond could be observed at 1640

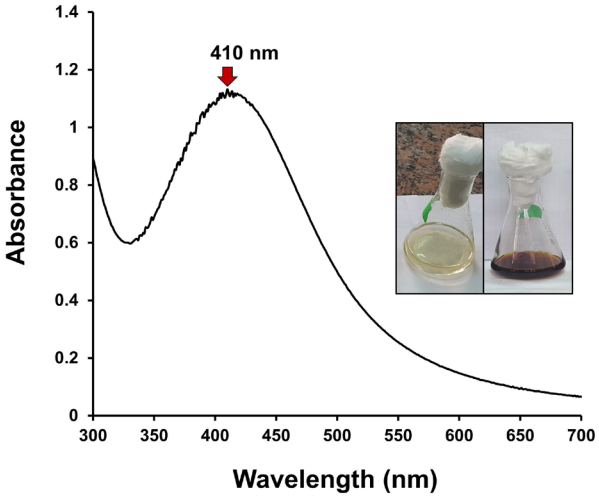

Figure 3: UV-Vis absorption spectrum of silver nanoparticles synthesized via *Albifimbria verrucaria* PRR$_2$.1 recorded at 410 nm, Figure 3 Insert on left-hand side showing the initial color of fungal-free filtrate and on the right-hand side demonstrating the change in color to reddish brown due to synthesis of silver nanoparticles.

which is characteristic to proteins. Sharp peak at 1043 cm^{-1} could be assigned to C-N stretch in proteins.

The XRD of silver nanoparticles synthesized by *A. verrucaria* PRR$_2$.1 exhibited four distinct Bragg reflections at 38.2, 44.5, 64.6 and 77.2 degrees corresponding to (111), (200), (220) and (311) orientations of crystal lattice planes of Face-centered cubic (fcc) silver (Figure 4g). The data obtained from XRD analysis of silver nanoparticles were matched with the Joint Committee on Powder Diffraction Standards (JCPDS) file No. 04-0783 confirming the crystalline nature of synthesized silver nanoparticles.

***In vitro* antimicrobial activity of biosynthesized silver nanoparticles**

Agar well diffusion method

Silver nanoparticles synthesized using *A. verrucaria* PRR$_2$.1 exhibited potent antimicrobial activity against tested human pathogens compared to that of antibiotic, antifungal and silver nitrate (100 µg/mL) (Table 2). The tested silver nanoparticles showed higher antifungal than antibacterial activity, with the highest activity against *C. albicans* and *A. niger*, while *E. coli* was the least susceptible among the tested pathogens. The fungal-free filtrate didn't possess any antimicrobial activity. Silver nitrate showed notable antimicrobial activity compared to silver nanoparticles but owing to its high cytotoxic effect on human cells (Hidalgo *et al.*, 1998), its antimicrobial activity was found insignificant. Figure 5 shows the antimicrobial activity of silver nanoparticles derived from *A. verrucaria* PRR$_2$.1 as zones of inhibition observed on Muller-Hinton agar.

 ISSN (print): 1823-8262, ISSN (online): 2231-7538

Malays. J. Microbiol. Vol 18(4) 2022, pp. 354-369
DOI: http://dx.doi.org/10.21161/mjm.221396

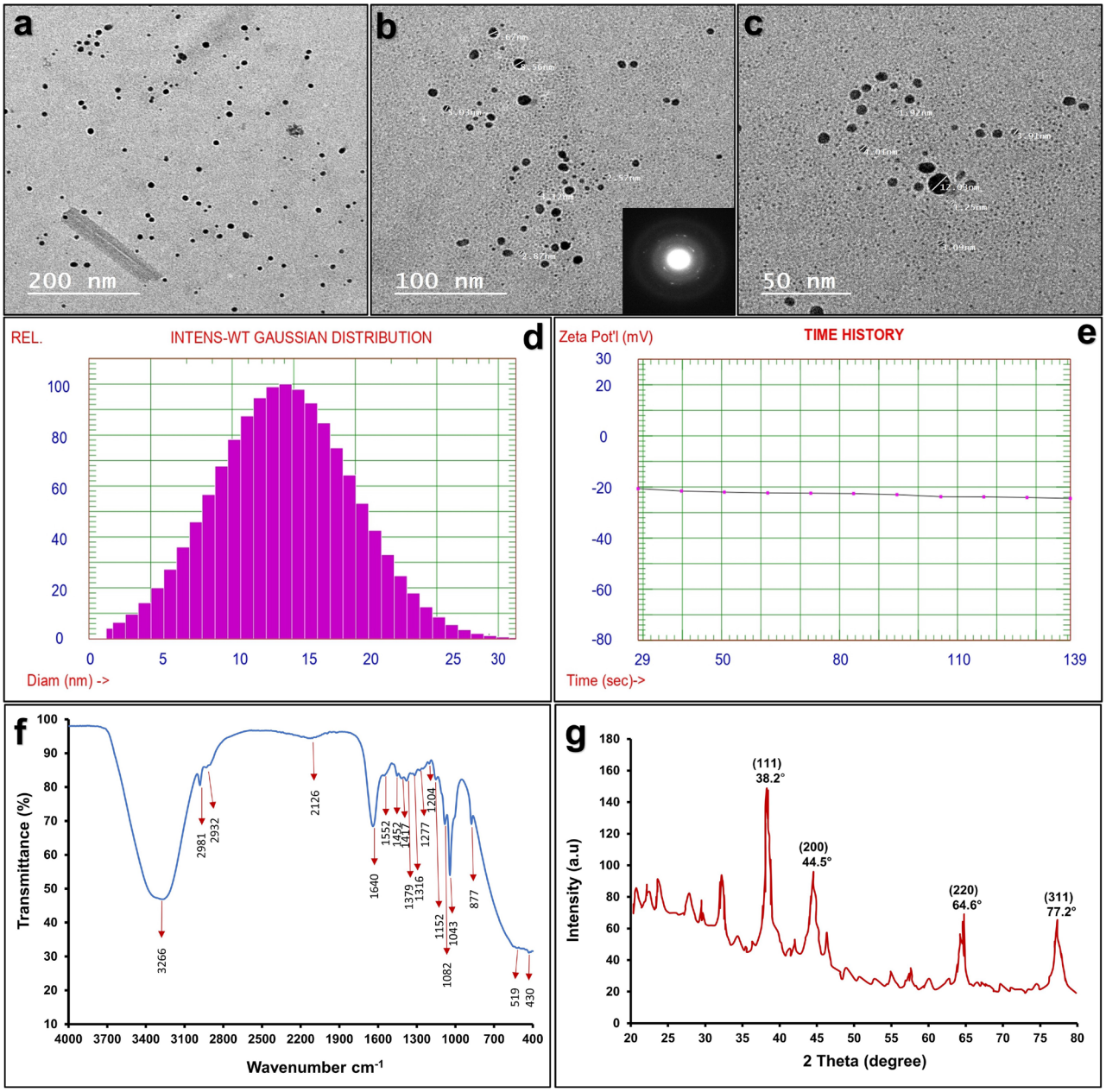

Figure 4: High resolution transmission electron microscopy **(**HR-TEM) micrographs of silver nanoparticles synthesized using *A. verrucaria* PRR$_2$.1, their Dynamic light scattering (DLS), Zeta-potential, Fourier transform infrared spectroscopy (FTIR) and X-ray diffraction pattern (XRD). (a, b and c) Different scales of HR-TEM micrographs of *A. verrucaria* PRR$_2$.1 synthesized silver nanoparticles with Figure 4b insert showing selected area electron diffraction (SAED) pattern. (d) *A. verrucaria* PRR$_2$.1 synthesized silver nanoparticles DLS histogram showing silver nanoparticles size distribution. (e) Zeta-potential of silver nanoparticles synthesized by *A. verrucaria* PRR$_2$.1. (f) FTIR spectroscopy of *A. verrucaria* PRR$_2$.1 synthesized SNPs. (g) XRD pattern of *A. verrucaria* PRR$_2$.1 synthesized SNPs.

Minimum inhibitory concentration

Minimum inhibitory concentration (MIC) was recorded visually as the lowest concentration of silver nanoparticles which completely inhibited the growth of tested microorganisms. MIC was recorded for silver nanoparticles synthesized using *A. verrucaria* PRR$_2$.1, antibiotic/antifungal and silver nitrate. Biosynthesized silver nanoparticles demonstrated more efficient and consistent antimicrobial activity at lower concentrations

 ISSN (print): 1823-8262, ISSN (online): 2231-7538

Malays. J. Microbiol. Vol 18(4) 2022, pp. 354-369
DOI: http://dx.doi.org/10.21161/mjm.221396

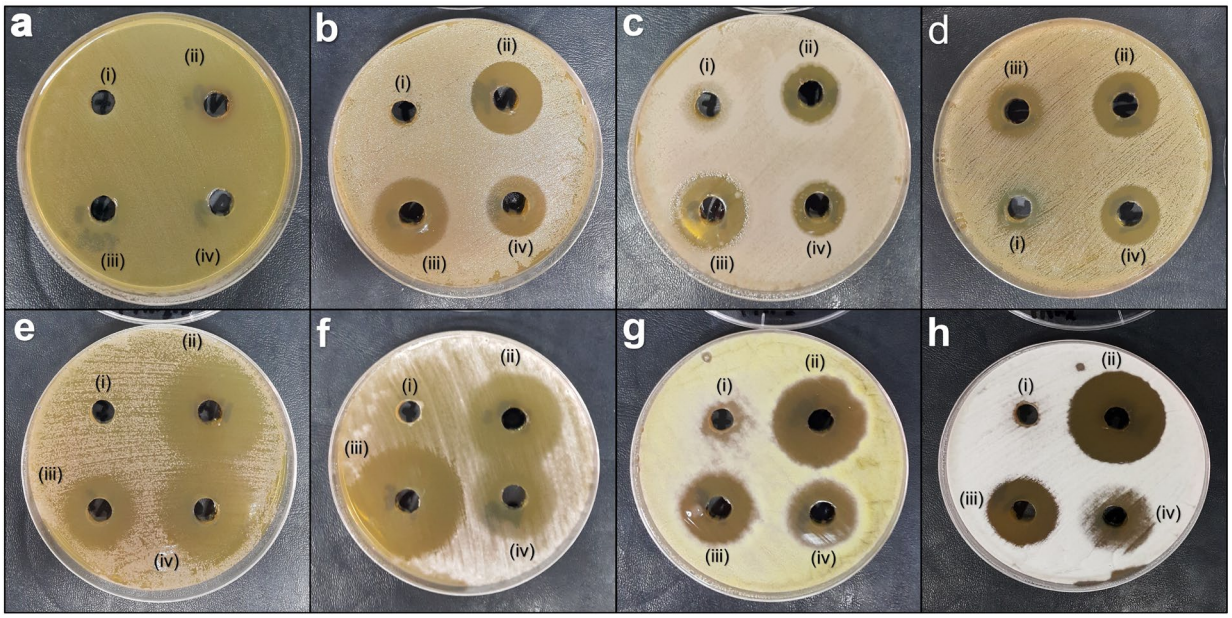

Figure 5: Antimicrobial activity of *A. verrucaria* PRR$_2$.1 synthesized silver nanoparticles against human pathogenic microorganisms by means of well diffusion assay showing zones of inhibition (ZOI). (a) *E. coli*, (b) *S. aureus*, (c) *B. cereus*, (d) *K. pneumonia*, (e) *C. albicans*, (f) *A. flavus*, (g) *A. niger* and (h) *A. fumigatus*. Each well treated with (i) Fungal biomass free filtrate (100 µL), (ii) Silver nanoparticles (170 µg/mL), (iii) Cefadroxil (100 µg/mL) and (iv) Silver nitrate (100 µg/mL).

Table 2: Antimicrobial activity and minimum inhibitory concentration (MIC) of silver nanoparticles derived from *Albifimbria verrucaria* PRR$_2$.1 against human pathogenic bacterial and fungal microorganisms.

Test pathogen	Diameter of inhibition zone (ZOI) (mm) / Minimum inhibitory concentration (MIC) (µg/mL)						
	Fungal free filtrate (100 µL)	Silver nanoparticles (170 µg/mL)		Cefadroxil/Itraconazole (100 µg/mL)		Silver nitrate (100 µg/mL)	
	ZOI	ZOI	MIC	ZOI	MIC	ZOI	MIC
E. coli	0	23	5.31	17	25	16	12.5
S. aureus	0	25	5.31	27	3.12	22	25
B. cereus	0	24	5.31	28	50	23	12.5
K. pneumoniae	0	24	5.31	20	25	20	25
C. albicans	0	35	10.62	22	12.5	31	25
A. flavus	0	34	5.31	38	12.5	28	12.5
A. niger	0	35	5.31	25	3.12	23	25
A. fumigatus	0	33	5.31	27	3.12	25	25

compared to that of antibiotic (Cefadroxil) except for *S. aureus*; antifungal (Itraconazole) except for *A. niger* and *A. fumigatus*; and silver nitrate (Table 2).

In vitro antiproliferative and cytotoxic activity of silver nanoparticles synthesized by *A. verrucaria* PRR$_2$.1

Antiproliferative activity of biosynthesized silver nanoparticles against HeLa cell line

The antitumor activity of silver nanoparticles synthesized by *A. verrucaria* PRR$_2$.1 was evaluated against HeLa cell line (cervical carcinoma cells) at different concentrations ranging from 0.78 to 100 µg/mL with IC_{50} (the concentration of silver nanoparticles that inhibits proliferation of HeLa cells by 50%) value equivalent to 2.52 ± 0.07 µg/mL after treatment for 48 h (Figure 6 and Table 3).

Cytotoxic activity of biosynthesized silver nanoparticles against WI-38 cell line

Similarly, the cytotoxic activity of silver nanoparticles synthesized by *A. verrucaria* PRR$_2$.1 was evaluated against WI-38 cell line (human lung fibroblast normal cells) at different concentrations ranging from 0.78 to 100 µg/mL with CC_{50} (the concentration of silver nanoparticles that causes the death of 50% of the tested cellular population) value equivalent to 10.2 ± 0.48 µg/mL after treatment for 48 h (Figure 6 and Table 3).

 ISSN (print): 1823-8262, ISSN (online): 2231-7538

Malays. J. Microbiol. Vol 18(4) 2022, pp. 354-369
DOI: http://dx.doi.org/10.21161/mjm.221396

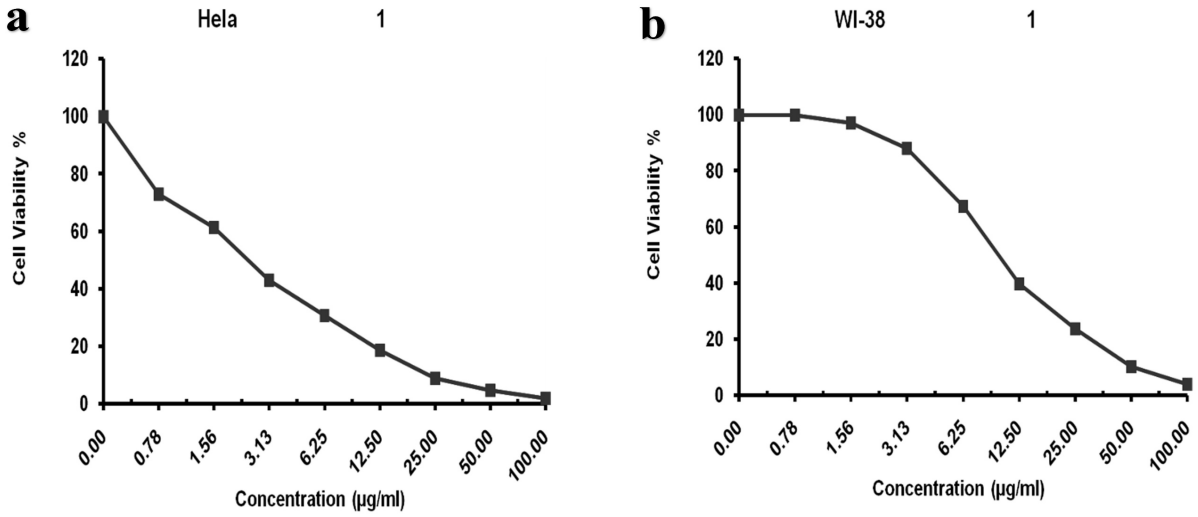

Figure 6: (a) Antiproliferative activity of silver nanoparticles synthesized using *A. verrucaria* PRR_2.1 against HeLa cell line. (b) Cytotoxic activity of silver nanoparticles synthesized using *A. verrucaria* PRR_2.1 WI-38 cell line.

Table 3: Antiproliferative and cytotoxic activity of silver nanoparticles synthesized by *Albifimbria verrucaria* PRR_2.1 against HeLa (cervical cancer) and WI-38 (normal human lung fibroblasts) cell lines.

SNPs concentration (µg/mL)	HeLa cells viability %	HeLa cells inhibitory %	WI-38 cells viability %	WI-38 cells inhibitory %
100	1.83	98.17	3.96	96.04
50	4.72	95.28	10.28	89.72
25	8.91	91.09	23.75	76.25
12.5	18.67	81.33	39.80	60.2
6.25	30.74	69.26	67.46	32.54
3.125	42.95	57.05	88.07	11.93
1.56	61.38	38.62	97.12	2.88
0.78	72.93	27.07	100	0
0	100	0	100	0

These results were detected using MTT assay with IC_{50} (2.52 ± 0.07 µg/mL after treatment for 48 h) against the HeLa cell line and CC_{50} (10.2 ± 0.48 µg/mL after treatment for 48 h) against WI-38 cell line values estimated from graphic plots of the dose-response curve for each concentration using GraphPad Prism software (San Diego, CA, USA).

DISCUSSION

Fungi are currently one of the most promising and frequently employed means for the extracellular biosynthesis of silver nanoparticles applicable in various fields, whether industrial, agricultural or biomedical, owing to their many advantages compared to other physical and chemical methods (Iravani *et al*., 2014). Ten samples were collected. Three soil samples were collected from different highly saline arid regions near Lake Moeris (Qarun Lake) in the northwest area of Faiyum Oasis located Southwest of Cairo Governorate, Egypt. The seven plants mentioned before were selected on the basis of their medicinal value (e.g., basil, mint, and fennel), their highly saline arid and subtropical habitat, which influence the nature of their endophytes such as their ability to produce a wide array of secondary metabolites to support their host plants in surviving these harsh habitat conditions. Three of which were collected from cultivated lands alongside Lake Moeris and the other 4 plant samples were collected from subtropical regions located in Wadi El-Rayan Protectorate, Faiyum Governorate, Egypt. These 10 samples yielded 60 fungal isolates which were all screened for their ability to biosynthesize silver nanoparticles. Among 21 isolates that were able to successfully support the biosynthesis of silver nanoparticles, the isolate identified as *Albifimbria verrucaria* PRR_2.1, an endophyte isolated from the roots of *O. basilicum* plant, was able to synthesize thermostable silver nanoparticles with long shelf-life without the tendency of aggregation. *Albifimbria verrucaria* PRR_2.1 optimally synthesized silver nanoparticles exhibited a strong UV-Vis absorption spectrum recorded at 410 nm as a result of their inherent surface plasmon resonance (Bindhu and Umadevi, 2013) depending on the size and shape of silver nanoparticles. The concentration of fungal biomass and silver nitrate greatly influences the size and concentration of silver nanoparticles produced. In the case of our study of silver nanoparticles synthesized using *A. verrucaria* PRR_2.1, the

 ISSN (print): 1823-8262, ISSN (online): 2231-7538

smallest size silver nanoparticles were obtained with 20 g/100 mL biomass concentration and 1.5 mM concentration of silver nitrate. This can be attributed to the fact that depending on the fungal species employed for the synthesis process; the successful synthesis of silver nanoparticles with desired physical and antimicrobial characteristics is the result of fine balance between the concentration of possible silver-reducing biomolecule(s) produced by employed fungal species and the amount of metal precursor available for synthesis (Phanjom and Ahmed, 2017; Shahzad *et al*., 2019). The abundance of organic biomolecule(s) responsible for the reduction of silver and biosynthesis of silver nanoparticles derived from 20 g/100 mL extract of *A. verrucaria* PRR_2.1, accompanied by low molar concentration of silver nitrate 1.5 mM as the metal precursor, efficiently enabled biosynthesis of smallest size silver nanoparticles with the highest stability and lower toxicity (Balakumaran *et al*., 2015; Phanjom and Ahmed, 2017; Elamawi *et al*., 2018).

It is well established that different growth media affect the growth rate of microorganisms as well as their ability to produce different metabolites and proteins (Costa Silva *et al*., 2017). PDB was the only growth medium to support the production of silver nanoparticles, while the other media tested (MGYPB, CDB and SDB) have completely inhibited the synthesis of silver nanoparticles. The same result was reported by Ashrafi *et al*. (2013), who have found that using MGYP as a growth medium for *Rhizoctonia solani* inhibited the production of silver nanoparticles, while the PDB medium successfully supported the synthesis process. This result suggests that media other than PDB or one of their components either inhibited the production or the activity of the enzyme responsible for the reduction of silver ions and formation of silver nanoparticles. The synthesis of silver nanoparticles using *A. verrucaria* PRR_2.1 favored alkaline pH. No change in color of the reaction mixture was observed and no UV-Vis absorption spectra were recorded at pH values less than pH 9, indicating inhibition of synthesis at lower pH values than pH 9 (Du *et al*., 2015; Othman *et al*., 2019). This can be attributed to the change in conformation of the enzyme responsible for the synthesis of nanoparticles at lower acidic pH rendering it inactive; also, it is worth noting that at higher pH, there is an increased competition between protons and positively charged silver ions to form bonds with negatively charged binding sites present in the silver-reducing enzyme (Sintubin *et al*., 2009). Temperature is one of the most influential parameters affecting the rate of synthesis and size of silver nanoparticles (Elamawi *et al*., 2018). The increase in incubation temperature of the reaction mixture up to 100 °C was accompanied by an increase in the rate of reaction and a blue shift in absorption spectra of synthesized silver nanoparticles, which indicates a decrease in size (Fayaz *et al*., 2009) with the smallest size observed at 60 °C. This indicates the thermal stability of biosynthesized silver nanoparticles at higher temperatures. This may be attributed to the fact that the formation of silver nanoparticles is a two-step process, the first step is the nucleation which includes the assembly of free silver atoms into a nucleus that serves as the core of newly growing silver nanoparticles, followed by growth which is the second step including deposition of more silver atoms around the nucleus forming the nanoparticle. Higher temperatures were found to enhance nucleation and inhibit the growth of formed nanoparticles which is the reason for the decrease in particle size (blue shift) with increased temperature (Liu *et al*., 2020). No color change of the reaction mixture was observed at 110 °C indicating failure of synthesis due to denaturation or inactivation of possible silver-reducing biomolecules(s) (Birla *et al*., 2013).

TEM micrographs showed well dispersed silver nanoparticles with sizes in agreement with that revealed by DLS; Zeta potential showed negatively charged silver nanoparticles which can be attributed to the role of possible reducing enzyme or other biomolecules in synthesis and stabilization of silver nanoparticles acting as a capping agent enclosing synthesized nanoparticles gaining them negative charge responsible for their stabilization by preventing agglomeration through electrostatic repulsion between particles (Gopinath *et al*., 2012). FTIR spectroscopy showed several bands corresponding to different functional groups present in possible biomolecules, including O-H (hydroxyl) group in alcohols, phenols and flavonoid compounds; C=O (carbonyl) stretch in N-C=O amide group of peptide bond which is characteristic to proteins, and C-N stretch in proteins which demonstrates the role of proteins and bioactive metabolites present in *A. verrucaria* PRR_2.1 filtrate in synthesizing and stabilization of silver nanoparticles (Chowdhury *et al*., 2014; Elgorban *et al*., 2016). XRD analysis confirmed the crystalline nature of silver nanoparticles in agreement with Joint Committee on Powder Diffraction Standards (JCPDS) file No. 04-0783.

Silver nanoparticles synthesized using *A. verrucaria* PRR_2.1 exhibited potent antimicrobial activity against all tested bacterial and fungal pathogens; the size and shape of silver nanoparticles impact their antimicrobial activity, as the smaller particles have a greater antimicrobial effect (Lu *et al*., 2013). Smaller particles can penetrate microbial cells more efficiently, causing several inhibitory mechanisms such as altering the permeability of cell wall and cell membrane, interfering with respiratory enzymes disabling respiratory chain reactions, and triggering the production of reactive oxygen species and free radicals, which damage cell membrane, interfering with DNA replication and cell division leading to cell death (Morones *et al*., 2005; Rai *et al*., 2009; Marambio-Jones and Hoek, 2010). The *in vitro* evaluation of *A. verrucaria* PRR_2.1 synthesized nanoparticles showed antiproliferative activity against the HeLa cell line at a low concentration with IC_{50} of 2.52 ± 0.07 µg/mL, which is a lower concentration than reported by other studies, including Rathod *et al*. (2016) and Abushiba *et al*. (2019) who have reported IC_{50} values against HeLa cell line of 6 µg/mL and 100 µg/mL, respectively. *A. verrucaria* PRR_2.1 synthesized SNPs have also relatively safe cytotoxic activity against WI-38 (human lung fibroblast) cell line with CC_{50} (the concentration of silver nanoparticles that causes the

 ISSN (print): 1823-8262, ISSN (online): 2231-7538

death of 50% of the tested cellular population) value equivalent to 10.2 ± 0.48 µg/mL relatively greater than IC_{50} against HeLa cell line, both of cell lines showed sensitivity to silver nanoparticles with HeLa cell line being more sensitive than WI-38 cell line. The *A. verrucaria* $PRR_{2.1}$ synthesized silver nanoparticles can be furtherly exploited as a potential anticancer and antioxidant agent. This brings us to the ratio known as selectivity index (SI), which is the ratio between CC_{50} affecting normal WI-38 cells divided by IC_{50} against HeLa cancerous cells; ideally, the tested antitumor agent should kill cancerous without affecting normal cells. In the case of *A. verrucaria* PRR_2.1 synthesized SNPs, the selectivity index equals 4, which is an acceptable value according to Weerapreeyakul *et al.* (2012) and Nogueira and Rosário (2010).

CONCLUSION

The data presented in this study show the potential of fungi, particularly endophytic fungal isolate *Albifimbria verrucaria* PRR_2.1 in the biosynthesis of thermostable silver nanoparticles as a possible biofriendly, safe and efficient antimicrobial agent with promising antiproliferative activity and low cytotoxic effect which can be furtherly implemented in various biomedical and biotechnological applications.

ACKNOWLEDGEMENTS

The first author would like to express his gratitude to Professor Dr. Adel Ahmed Ramadan El-Mehalawy, Dr. Samar Samir Mohamed and Dr. Noha Mohamed Abd Elhameed (Department of Microbiology, Faculty of Science, Ain Shams University, Cairo, Egypt) for their continuous guidance, help and support.

CONFLICT OF INTEREST

The authors have no conflicts of interest to declare relevant to this article's content.

REFERENCES

Abdel-Rahim, K., Mahmoud, S. Y., Ali, A. M., Almaary, K. S., Mustafa, A. E. Z. and Husseiny, S. M. (2017). Extracellular biosynthesis of silver nanoparticles using *Rhizopus Stolonifer*. *Saudi Journal of Biological Sciences* **24(1), 208-216.**

Abushiba, M., El-Sherbiny, G., Moghannem, S., Kalaba, M., El-Shatoury, E. and Saeed, A. (2019). Enhancement of antibiotics activity by microbially synthesized silver nanoparticles. *African Journal of Biological Sciences* **15(1), 137-153.**

Adeeyo, A. O. and Odiyo, J. O. (2018). Biogenic synthesis of silver nanoparticle from mushroom exopolysaccharides and its potentials in water purification. *Open Chemistry Journal* **5, 64-75.**

Ahmad, N., Bhatnagar, S., Ali, S. S. and Dutta, R. (2015). Phytofabrication of bioinduced silver nanoparticles for biomedical applications. *International Journal of Nanomedicine* **10, 7019-7030.**

Ashrafi, S. J., Rastegar, M. F., Ashrafi, M., Yazdian, F., Pourrahim, R. and Suresh, A. K. (2013). Influence of external factors on the production and morphology of biogenic silver nanocrystallites. *Journal of Nanoscience and Nanotechnology* **13(3), 2295-2301.**

Balakumaran, M. D., Ramachandran, R., Balashanmugam, P., Mukeshkumar, D. J. and Kalaichelvan, P. T. (2016). Mycosynthesis of silver and gold nanoparticles: Optimization, characterization and antimicrobial activity against human pathogens. *Microbiological Research* **182, 8-20.**

Balakumaran, M. D., Ramachandran, R. and Kalaichelvan, P. T. (2015). Exploitation of endophytic fungus, *Guignardia mangiferae* for extracellular synthesis of silver nanoparticles and their *in vitro* biological activities. *Microbiological Research* **178, 9-17.**

Balouiri, M., Sadiki, M. and Ibnsouda, S. K. (2016). Methods for *in vitro* evaluating antimicrobial activity: A review. *Journal of Pharmaceutical Analysis* **6(2), 71-79.**

Basavaraja, S., Balaji, S. D., Lagashetty, A., Rajasab, A. H. and Venkataraman, A. (2008). Extracellular biosynthesis of silver nanoparticles using the fungus *Fusarium semitectum*. *Materials Research Bulletin* **43(5), 1164-1170.**

Baymiller, M., Huang, F. and Rogelj, S. (2017). Rapid one-step synthesis of gold nanoparticles using the ubiquitous coenzyme NADH. *Matters* **2017, 1-4.**

Bhangale, H. G., Bachhav, S. G., Nerkar, D. M., Sarode, K. M. and Patil, D. R. (2019). Study on optical properties of green synthesized silver nanoparticles for surface plasmon resonance. *Journal of Nanoscience and Technology* **5(2), 658-661.**

Bindhu, M. R. and Umadevi, M. (2013). Green synthesized gold nanoparticles as a probe for the detection of Fe^{3+} ions in water. *Journal of Cluster Science* **25(4), 969-978.**

Birla, S. S., Gaikwad, S. C., Gade, A. K. and Rai, M. K. (2013). Rapid synthesis of silver nanoparticles from *Fusarium oxysporum* by optimizing physicocultural conditions. *Scientific World Journal* **2013, Article ID 796018.**

Burdușel, A., Gherasim, O., Grumezescu, A. M., Mogoantă, L., Ficai, A. and Andronescu, E. (2018). Biomedical applications of silver nanoparticles: An up-to-date overview. *Nanomaterials* **8(9), 681.**

Chowdhury, S., Basu, A. and Kundu, S. (2014). Green synthesis of protein capped silver nanoparticles from phytopathogenic fungus *Macrophomina phaseolina* (Tassi) Goid with antimicrobial properties against multidrug-resistant bacteria. *Nanoscale Research Letters* **9, 365.**

Costa Silva, L. P., Oliveira, J. P., Keijok, W. J., da Silva, A. R., Aguiar, A. R., Guimarães, M. C. C., Ferraz, C. M., Araújo, J. V., Tobias, F. L. and Braga, F. R. (2017). Extracellular biosynthesis of silver

nanoparticles using the cell-free filtrate of nematophagous fungus *Duddingtonia flagrans*. *International Journal of Nanomedicine* **12, 6373-6381.**

Crous, P. W., Petrini, O., Marais, G. F., Pretorius, Z. A. and Rehder, F. (1995). Occurrence of fungal endophytes in cultivars of *Triticum aestivum* in South Africa. *Mycoscience* **36(1), 105-111.**

Dhabalia, D., Ukkund, S. J., Syed, U. T., Uddin, W. and Kabir, M. A. (2020). Antifungal activity of biosynthesized silver nanoparticles from *Candida albicans* on the strain lacking the *CNP*41 gene. *Materials Research Express* **7(12), 125401.**

Du, L., Xu, Q., Huang, M., Xian, L. and Feng, J. X. (2015). Synthesis of small silver nanoparticles under light radiation by fungus *Penicillium oxalicum* and its application for the catalytic reduction of methylene blue. *Materials Chemistry and Physics* **160, 40-47.**

Duval, R. E., Grare, M. and Demoré, B. (2019). Fight against antimicrobial resistance: We always need new antibacterials but for right bacteria. *Molecules* **24(17), 3152.**

Elamawi, R. M., Al-Harbi, R. E. and Hendi, A. A. (2018). Biosynthesis and characterization of silver nanoparticles using *Trichoderma longibrachiatum* and their effect on phytopathogenic fungi. *Egyptian Journal of Biological Pest Control* **28, 28.**

El-Eraky, A. M. I., Moubasher, A. H., Ismail, M. A., El-Shaer, A. H. and Gouda, H. A. (2017). Mycosynthesis of silver nanoparticles and their role in the control of *Fusarium* wilt of pepper. *Journal of Basic and Applied Mycology* **8, 25-34.**

Elgorban, A. M., Aref, S. M., Seham, S. M., Elhindi, K. M., Bakhali, A. H., Sayed, S. R. and Manal, M. A. (2016). Extracellular synthesis of silver nanoparticles using *Aspergillus versicolor* and evaluation of their activity on plant pathogenic fungi. *Mycosphere* **7(6), 844-852.**

El-Sayed, E. R., Abdelhakim, H. K. and Zakaria, Z. (2020). Extracellular biosynthesis of cobalt ferrite nanoparticles by *Monascus purpureus* and their antioxidant, anticancer and antimicrobial activities: Yield enhancement by gamma irradiation. *Materials Science and Engineering: C* **107, 110318.**

Farsi, M. and Farokhi, S. (2018). Biosynthesis of antibacterial silver nanoparticles by endophytic fungus *Nemania* sp. isolated from *Taxus baccata* L. (Iranian Yew). *Zahedan Journal of Research in Medical Sciences* **20(6), e57916.**

Fayaz, A. M., Balaji, K., Kalaichelvan, P. T. and Venkatesan, R. (2009). Fungal based synthesis of silver nanoparticles — An effect of temperature on the size of particles. *Colloids and Surfaces B: Biointerfaces* **74(1), 123-126.**

Ghareib, M., Tahon, M. A., Saif, M. M. and Abdallah, W. E. (2016). Rapid extracellular biosynthesis of silver nanoparticles by *Cunninghamella phaeospora* culture supernatant. *Iranian Journal of Pharmaceutical Research* **15(4), 915-924.**

Gopinath, V., MubarakAli, D., Priyadarshini, S., Priyadharsshini, N. M., Thajuddin, N. and Velusamy, P. (2012). Biosynthesis of silver nanoparticles from *Tribulus terrestris* and its antimicrobial activity: A novel biological approach. *Colloids and Surfaces B: Biointerfaces* **96, 69-74.**

Gudikandula, K., Vadapally, P. and Charya, M. A. S. (2017). Biogenic synthesis of silver nanoparticles from white rot fungi: Their characterization and antibacterial studies. *OpenNano* **2, 64-78.**

Guilger-Casagrande, M. and de Lima, R. (2019). Synthesis of silver nanoparticles mediated by fungi: A review. *Frontiers in Bioengineering and Biotechnology* **7, 287.**

Hidalgo, E., Bartolomé, R., Barroso, C., Moreno, A. and Domínguez, C. (1998). Silver nitrate: Antimicrobial activity related to cytotoxicity in cultured human fibroblasts. *Skin Pharmacology and Applied Skin Physiology* **11(3), 140-151.**

Hietzschold, S., Walter, A., Davis, C., Taylor, A. A. and Sepunaru, L. (2019). Does nitrate reductase play a role in silver nanoparticle synthesis? Evidence for NADPH as the sole reducing agent. *ACS Sustainable Chemistry and Engineering* **7(9), 8070-8076.**

Iravani, S., Korbekandi, H., Mirmohammadi, S. V. and Zolfaghari, B. (2014). Synthesis of silver nanoparticles: Chemical, physical and biological methods. *Research in Pharmaceutical Sciences* **9(6), 385-406.**

Jebril, S., Jenana, R. K. B. and Dridi, C. (2020). Green synthesis of silver nanoparticles using *Melia azedarach* leaf extract and their antifungal activities: *In vitro* and *in vivo*. *Materials Chemistry and Physics* **248, 122898.**

Jyoti, K., Baunthiyal, M. and Singh, A. (2016). Characterization of silver nanoparticles synthesized using *Urtica dioica* Linn. leaves and their synergistic effects with antibiotics. *Journal of Radiation Research and Applied Sciences* **9(3), 217-227.**

Kathiresan, K., Manivannan, S., Nabeel, M. A. and Dhivya, B. (2009). Studies on silver nanoparticles synthesized by a marine fungus, *Penicillium fellutanum* isolated from coastal mangrove sediment. *Colloids and Surfaces B: Biointerfaces* **71(1), 133-137.**

Khandel, P. and Shahi, S. K. (2018). Mycogenic nanoparticles and their bio-prospective applications: Current status and future challenges. *Journal of Nanostructure in Chemistry* **8, 369-391.**

Khatoon, N., Mazumder, J. A. and Sardar, M. (2017). Biotechnological applications of green synthesized silver nanoparticles. *Journal of Nanosciences: Current Research* **2, 107.**

Lee, S. H. and Jun, B. H. (2019). Silver nanoparticles: Synthesis and application for nanomedicine. *International Journal of Molecular Sciences* **20(4), 865.**

Liu, H., Zhang, H., Wang, J. and Wei, J. (2020). Effect of temperature on the size of biosynthesized silver nanoparticle: Deep insight into microscopic kinetics analysis. *Arabian Journal of Chemistry* **13, 1011-1019.**

Lu, Z., Rong, K., Li, J., Yang, H. and Chen, R. (2013). Size-dependent antibacterial activities of silver

nanoparticles against oral anaerobic pathogenic bacteria. *Journal of Materials Science: Materials in Medicine* **24(6), 1465-1471.**

Manikandaselvi, S., Sathya, V., Vadivel, V., Sampath, N. and Brindha, P. (2020). Evaluation of bio control potential of AgNPs synthesized from *Trichoderma viride*. *Advances in Natural Sciences: Nanoscience and Nanotechnology* **11(3), 035004.**

Marambio-Jones, C. and Hoek, E. M. V. (2010). A review of the antibacterial effects of silver nanomaterials and potential implications for human health and the environment. *Journal of Nanoparticle Research* **12(5), 1531-1551.**

Mishra, A., Kumari, M., Pandey, S., Chaudhry, V., Gupta, K. C. and Nautiyal, C. S. (2014). Biocatalytic and antimicrobial activities of gold nanoparticles synthesized by *Trichoderma* sp. *Bioresource Technology* **166, 235-242.**

Morones, J. R., Elechiguerra, J. L., Camacho, A., Holt, K., Kouri, J. B., Ramírez, J. T. and Yacaman, M. J. (2005). The bactericidal effect of silver nanoparticles. *Nanotechnology* **16(10), 2346-2353.**

Mosmann, T. (1983). Rapid colorimetric assay for cellular growth and survival: Application to proliferation and cytotoxicity assays. *Journal of Immunological Methods* **65(1-2), 55-63.**

Moubasher, A. H. (1993). Soil Fungi in Qatar and Other Arab Countries. Centre for Scientific and Applied Research, University of Qatar, Doha, Qatar.

Mousa, S. A., El-Sayed, E. R., Mohamed, S. S., Abo El-Seoud, M. A., Elmehlawy, A. A. and Abdou, D. A. (2021). Novel mycosynthesis of Co_3O_4, CuOo, Fe_3O_4, NiO, and ZnO nanoparticles by the endophytic *Aspergillus terreus* and evaluation of their antioxidant and antimicrobial activities. *Applied Microbiology and Biotechnology* **105(2), 741-753.**

Nogueira, F. and Rosário, V. E. (2010). Methods for assessment of antimalarial activity in the different phases of the *Plasmodium* life cycle. *Revista Pan-Amazônica de Saúde* **1(3), 109-124.**

Othman, A. M., Elsayed, M. A., Al-Balakocy, N. G., Hassan, M. M. and Elshafei, A. M. (2019). Biosynthesis and characterization of silver nanoparticles induced by fungal proteins and its application in different biological activities. *Journal of Genetic Engineering and Biotechnology* **17, 8.**

Pelhate, J. (1968). Contribution to the Ecological Study of Molds in Storage Wheat. Salt Lake, Utah.

Petrikkou, E., Rodríguez-Tudela, J. L., Cuenca-Estrella, M., Gómez, A., Molleja, A. and Mellado, E. (2001). Inoculum standardization for antifungal susceptibility testing of filamentous fungi pathogenic for humans. *Journal of Clinical Microbiology* **39(4), 1345-1347.**

Phanjom, P. and Ahmed, G. (2017). Effect of different physicochemical conditions on the synthesis of silver nanoparticles using fungal cell filtrate of *Aspergillus oryzae* (MTCC No. 1846) and their antibacterial effect. *Advances in Natural Sciences: Nanoscience and Nanotechnology* **8(4), 045016.**

Pongtharangkul, T. and Demirci, A. (2004). Evaluation of agar diffusion bioassay for nisin quantification. *Applied Microbiology and Biotechnology* **65(3), 268-272.**

Rai, M., Bonde, S., Golinska, P., Trzcińska-Wencel, J., Gade, A., Abd-Elsalam, K. A., Shende, S., Gaikwad, S. and Ingle, A. P. (2021). *Fusarium* as a novel fungus for the synthesis of nanoparticles: Mechanism and applications. *Journal of Fungi* **7(2), 139.**

Rai, M., Yadav, A. and Gade, A. (2009). Silver nanoparticles as a new generation of antimicrobials. *Biotechnology Advances* **27(1), 76-83.**

Rathod, D., Golinska, P., Wypij, M., Dahm, H. and Rai, M. (2016). A new report of *Nocardiopsis valliformis* strain OT1 from alkaline Lonar crater of India and its use in synthesis of silver nanoparticles with special reference to evaluation of antibacterial activity and cytotoxicity. *Medical Microbiology and Immunology* **205(5), 435-447.**

Rauwel, P., Küünal, S., Ferdov, S. and Rauwel, E. (2015). A review on the green synthesis of silver nanoparticles and their morphologies studied via TEM. *Advances in Materials Science and Engineering* **2015, Article ID 682749.**

Saxena, J., Sharma, P. K., Sharma, M. M. and Singh, A. (2016). Process optimization for green synthesis of silver nanoparticles by *Sclerotinia sclerotiorum* MTCC 8785 and evaluation of its antibacterial properties. *SpringerPlus* **5(1), 861.**

Seetharaman, P. K., Chandrasekaran, R., Gnanasekar, S., Chandrakasan, G., Gupta, M., Manikandan, D. B. and Sivaperumal, S. (2018). Antimicrobial and larvicidal activity of eco-friendly silver nanoparticles synthesized from endophytic fungi *Phomopsis liquidambaris*. *Biocatalysis and Agricultural Biotechnology* **16, 22-30.**

Shahzad, A., Saeed, H., Iqtedar, M., Hussain, S. Z., Kaleem, A., Abdullah, R., Sharif, S., Naz, S., Saleem, F., Aihetasham, A. and Chaudhary, A. (2019). Size-controlled production of silver nanoparticles by *Aspergillus fumigatus* BTCB10: Likely antibacterial and cytotoxic effects. *Journal of Nanomaterials* **2019, Article ID 5168698.**

Sieber, T., Riesen, T. K., Müller, E. and Fried, P. M. (1988). Endophytic fungi in four winter wheat cultivars (*Triticum aestivum* L.) differing in resistance against *Stagonospora Nodorum* (Berk.) cast. & Germ. = *Septoria nodorum* (Berk.) Berk. *Journal of Phytopathology* **122(4), 289-306.**

Singh, A. K., Rathod, V., Singh, D., Ninganagouda, S., Kulkarni, P., Mathew, J. and Ul-Haq, M. (2015). Bioactive silver nanoparticles from endophytic fungus *Fusarium* sp. isolated from an ethanomedicinal plant *Withania somnifera* (Ashwagandha) and its antibacterial activity. *International Journal of Nanomaterials and Biostructures* **5(1), 15-19.**

Singh, R., Wagh, P., Wadhwani, S., Gaidhani, S., Kumbhar, A., Bellare, J. and Chopade, B. A. (2013). Synthesis, optimization, and characterization of silver nanoparticles from *Acinetobacter calcoaceticus* and

their enhanced antibacterial activity when combined with antibiotics. *International Journal of Nanomedicine* **8(1), 4277-4290.**

Sintubin, L., De Windt, W., Dick, J., Mast, J., van der Ha, D., Verstraete, W. and Boon, N. (2009). Lactic acid bacteria as reducing and capping agent for the fast and efficient production of silver nanoparticles. *Applied Microbiology and Biotechnology* **84(4), 741-749.**

Su, H., Han, L. and Huang, X. (2018). Potential targets for the development of new antifungal drugs. The *Journal of Antibiotics* **71(12), 978-991.**

Tyagi, S., Tyagi, P. K., Gola, D., Chauhan, N. and Bharti, R. K. (2019). Extracellular synthesis of silver nanoparticles using entomopathogenic fungus: Characterization and antibacterial potential. *SN Applied Sciences* **1, 1545.**

Wang, D., Xue, B., Wang, L., Zhang, Y., Liu, L. and Zhou, Y. (2021). Fungus-mediated green synthesis of nano-silver using *Aspergillus sydowii* and its antifungal/antiproliferative activities. *Scientific Reports* **11, 10356.**

Weaver, M. A., Hoagland, R. E., Boyette, C. D. and Brown, S. P. (2021). Taxonomic evaluation of a bioherbicidal isolate of *Albifimbria verrucaria*, formerly *Myrothecium verrucaria*. *Journal of Fungi* **7(9), 694.**

Weerapreeyakul, N., Nonpunya, A., Barusrux, S., Thitimetharoch, T. and Sripanidkulchai, B. (2012). Evaluation of the anticancer potential of six herbs against a hepatoma cell line. *Chinese Medicine* **7, 15.**

White, T. J., Bruns, T., Lee, S. and Taylor, J. (1990). Amplification and direct sequencing of fungal ribosomal RNA genes for phylogenetics. *In*: PCR Protocols: A Guide to Methods and Applications. Innis, M. A., Gelfand, D. H., Sninsky, J. J. and White, T. J. (eds.). Academic Press, San Diego, USA. **pp. 315-322.**

 ISSN (print): 1823-8262, ISSN (online): 2231-7538